Lithuanian Journal of Physics, Vol. **61**, No. 2, pp. 97–109 (2021)

PHOTO-ACOUSTIC RESPONSE AND OPTICAL FEATURES OF 2D-$TlGaSe_2$ AND GaAs SEMICONDUCTORS

V. Grivickas [a], K. Gulbinas [a], V. Bikbajevas [a], and P. Grivickas [b]

[a] *Institute of Photonics and Nanotechnology, Vilnius University, Saulėtekio 3, 10257 Vilnius, Lithuania*

[b] *Lawrence Livermore National Laboratory, Livermore, CA 94550 USA*

Email: vytautas.grivickas@ff.vu.lt

Received 14 May 2021; accepted 18 May 2021

The paper focuses on investigation of the acoustic-optical properties of 2D-$TlGaSe_2$ and GaAs semiconductors using laser pulses. We present the photo-darkening experiments performed by using CW light in spectral ranges below the band gap of $TlGaSe_2$. The data provides evidence that photo-acoustic signals (PAS) for the above band gap are significantly stronger and linear in 2D-$TlGaSe_2$ while they are distorted by nonlinear processes in isotropic GaAs. The comparison discloses characteristic parameters of $TlGaSe_2$, namely a high factor and a negative sign in the refraction coefficient with pressure, a low absorption coefficient and absence of band filling; all guarantee stabile energy conversion by thermoelastic deformation mechanism. Below the band gap range, we found a new kind of PAS in $TlGaSe_2$ on near surfaces. Likewise, we demonstrate that in such spectral range the giant Stark effect in $TlGaSe_2$ is created by focused CW beams. The Stark effect produces local optical darkening which can provide explosion at extreme light power. Likely, both effects could be related to the planar stacking faults in 2D-$TlGaSe_2$, which produce a spontaneous charge separation on layers.

Keywords: 2D-semiconductors, optical deflection, photo-acoustics, induced Stark effect, photo-darkening

PACS: 78.20, 43.35

1. Introduction

Two-dimensional (2D) multi-layered dichalcogenide semiconductor $TlGaSe_2$ has been known for a long time [1, 2]. The compound crystallizes in the monoclinic symmetry group $C2/c$–C^6_{2h} with the unit cell parameter a = 10.771 Å, b = 10.772 Å, c = 15.64 Å and the main crystallographic c^* axis directed at monoclinic angle β = 100.06°. The unit cell contains 16 atoms positioned on two adjacent layers rotated by 90° angle in (100) plain. The Tl atoms lie in perpendicular trigonal cavities between layers and provide a weak interlayer covalent bonding [1, 3–7]. Due to the sufficient length of these bonds, there is a predisposition for electrical anisotropy. It was experimentally shown that the ratio of conductivity along and normal to the layers $\sigma^0_{\parallel}/\sigma^0_{\perp}$ varies in a range of 10^3–10^8 [1].

In recent years, $TlGaSe_2$ and $TlInS_2$ compounds have gained significant interest because of discovering their unique, unexpected electro-optical properties. In conjunction with previously known sequential phase transitions occurring at low temperatures, extensively studied during last decades [1, 3, 4], recent investigation indicated electro-optical metastable transformations if samples were thermo-cycled or kept for a certain period in the external electric fields (see [5] and references therein). Our previous works have shown that $TlGaSe_2$ as well as the equivalent $TlInS_2$ compound obey phenomena of temporal or permanent photo-darkening (giant Stark effect) after a prolonged intense laser pulse irradiation [6, 7]. Moreover, we demonstrated physical evidence that the periodic electron–hole (e–h) charge separation on the layer plain occurs at any excitation event by

self-charge trapping and a small variation in the band gap [6, 7]. Likely, this effect is much perturbed with the mismatch of layer structure by presence of planar stacking faults (PSF).

The photo-acoustic responses from $TlGaSe_2$ [8] and layered van der Waals GaSe semiconductor has been observed in [9]. These measurements were performed by the so-called Schlieren optical deflection technique [10]. However, no reasonable explanation of acoustic phenomena was produced in a frame of new knowledge on layered 2D compounds.

In this work, we present the photo-acoustic investigation in the $TlGaSe_2$ taking opportunity of comparison with a parallel detection by the same technique for isotropic GaAs which is a vital semiconductor in state-of-the-art acoustic investigations (see [11] and citations therein). This allows understanding of the acousto-optic mechanism for the above and the below bad gap excitations. The results are presented in accordance with the measurements of photo-darkening phenomena in $TlGaSe_2$ at energy below the band gap. We demonstrate that planar stacking faults likely induce a specific PAS response in the 2D-$TlGaSe_2$ structure. We suggest that PSFs affect the generation of the giant Stark effect by CW light sub-gap irradiation.

2. Experiment

The $TlGaSe_2$ crystals were grown by a modified Bridgman method wherein high purity elements in a furnace are taken in stoichiometric proportions [4]. We characterized the grown $TlGaSe_2$ crystals by X-ray and photoluminescence (PL) spectroscopy, Hall measurements, hot-probe technique and more closely by optical spectroscopy [4, 7]. Modelling of the absorption edge showed that the lowest direct exciton bandgap was equal to E_{gx}^{d} = 2.117 eV with the exciton binding energy E_{x}^{d} = 28 meV while the indirect exciton bandgap was equal to E_{gx}^{i} = 2.08 eV at 295 K [7]. Sufficient damping of the direct oscillator strength was detected allowing quite low absorption coefficients. It was shown that excitons are substantially polarized across the layers [4]. For current photo-acoustic experiments, a careful gentle polishing of the $TlGaSe_2$ sample was performed on lateral sides with a final front cleavage to sustain corners of the damaged part at (001) facets. Allowable slabs were of 0.3 × 1.8 × 4 mm dimension.

The GaAs was chosen because it is a well-established semiconductor in the photo-acoustic studies with femtosecond-to-nanosecond duration laser pulses on a wide spectral range [11, 12]. The GaAs samples were obtained from a high quality two-inch double polished 0.5 mm thick (100) commercial wafer with an impurity content below 10^{15} cm^{-3}. The lateral mirror sides were produced by breaking a wafer along the (100) direction. Optical inspection showed that the lateral sides make mirror image surfaces. The slab dimension was 0.5 × 1.5 × 8 mm.

Figure 1(a) shows the experimental setup with significant details of a measuring apparatus. The Q-switched Infinity (*Coherent*) Nd:YAG seeded laser is used as the excitation source. It generates high energy pulses of 2 ns duration at 40 Hz repetition rate. The fundamental first harmonic passes the second harmonic generation (SHG) crystal and then the third harmonic generation (THG) crystal to triple output photon energy. To obtain tunable wavelength light, the third harmonic is sent to opto-parametric optical (OPO) crystals where two beams are generated: the signal and the idler. The signal is varied through a range of 430–710 nm wavelength and the idler can be tuned in the interval 710–1600 nm. The value of wavelength is controlled by a computer. The output light wavelength was calibrated using an external Ocean spectrometer and a Hg lamp. The laser light was linearly polarized by a Berek rotator.

The probe-beam was set by a number of CW light lasers, which were focused on the sample surface in a spot with 5–20 μm diameter [13]. The transmitted probe light was collimated by two lenses onto a 0.5 ns rise time InGaAs photo-receiver. The signals were detected by a 2 GHz oscilloscope and recorded by PC. Typically, 500 results were averaged to increase the signal-to-noise ratio. The samples were placed in an optical cryostat, the holder of which allowed its fine moving in a few directions in respect to the pump and probe beam crossing. The driving motor allowed shifting the probe beam any distance from the excited surface with sub-micron precision.

To study the photo-darkening by CW laser irradiation, irradiations were exposed onto the spots at normal direction to the layer plane (100) in $TlGaSe_2$.

In these experiments, optical filters were used to reduce/increase the irradiation power. The measurements were performed in air or in vacuum under different irradiation sequences. The transmitted intensity was detected in real time during the laser exposure developing the darkening. A detailed mapping scan of the darkening area was performed on the sample after the irradiation period by the same wavelength or by another beam wavelength. This excitation was carried out under intensity low enough to avoid further darkening process (or annealing). If the darkening was permanent, the images were analysed by an optical microscope.

3. PAS formation and detection

We consider the longitudinal plane acoustic wave generated in the slab near the excited front surface as shown in Fig. 1(b). When the laser pulse excites the facial layer, some energy is absorbed inside the slab. For the free (unbound) surface the material reaction is provided by thermal expansion in a small area in which the boundary strain at surface $z = 0$ is maintained at zero. This particular case is used throughout the experiments presented below. Therefore, the bipolar PAS in the form of acoustic wave is generated due to the free surface reaction to

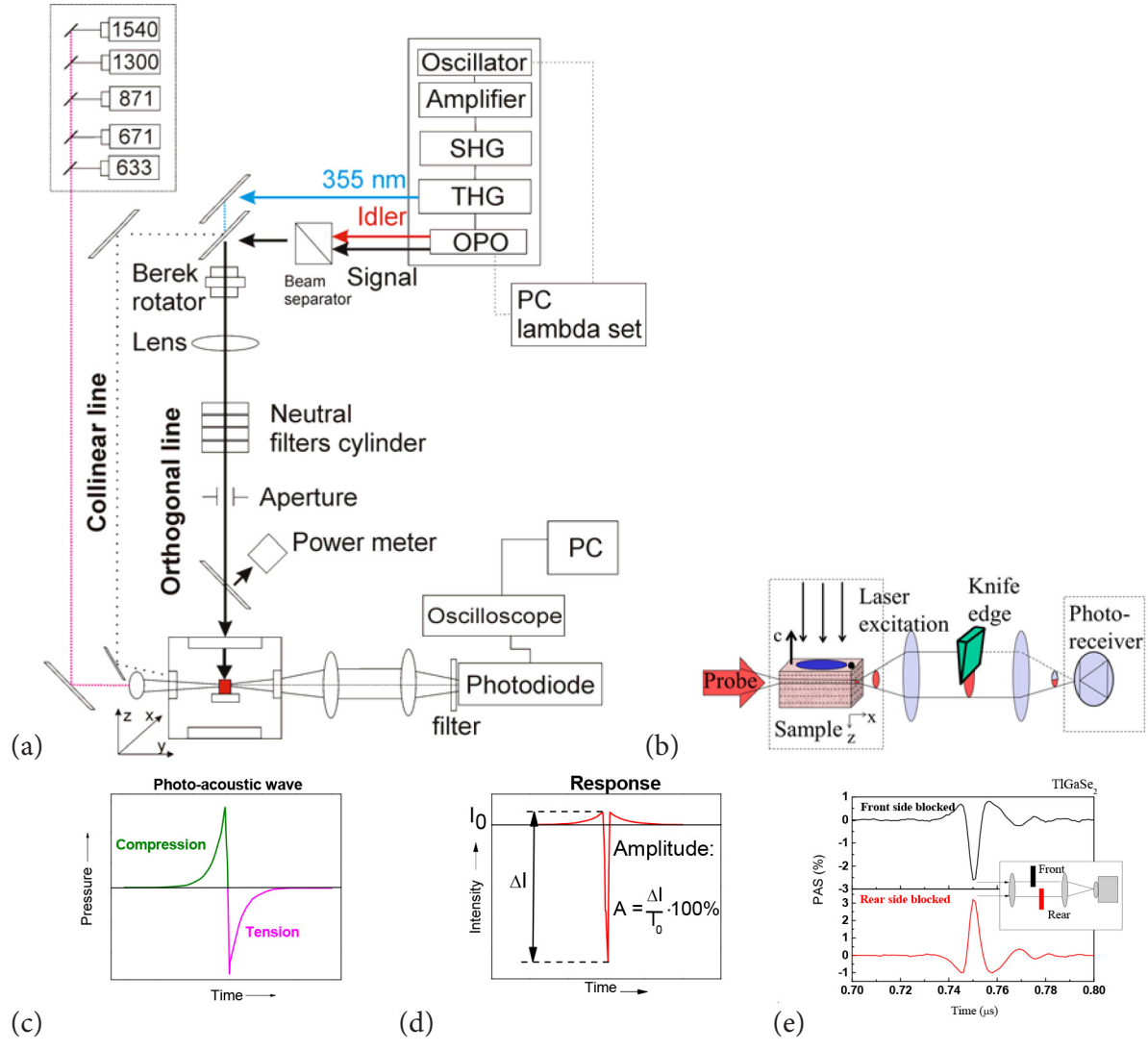

Fig. 1. (a) Pump-probe measurement setup with a 2 ns pulse pump laser. Values of CW probe wavelengths in nanometres are indicated in the top-left corner. (b) The Schlieren detection scheme for a perpendicular probe beam by clipping the beam across with the knife edge. (c) The theoretical PA wave profile propagating from the excited surface. (d) The derivative of PAS which accounts for the refractive index variation by acoustic pressure. (e) Experimental signals from the $TlGaSe_2$ slab with the opposite position of the inserted knife. Coloured online.

pulse energy absorption (Fig. 1(c) [10]). Two mechanisms of PAS formation should be considered seriously in the case of a semiconductor: the thermoelastic process as a result of laser pulse absorption, and the deformation mechanism which is based on the change of electronic volume as a result of e–h pair generation [12, 14]. One-dimensional equation for such lattice displacements can be solved analytically [14]. The time dependence of surface strain is expressed as

$$\eta_{zz}(0,t) = \frac{1}{\rho v_{ac}^2}[3B\beta\Delta T(0,t) - d_{eh}n(0,t)], \qquad (1)$$

where B is the bulk modulus, β is the thermal expansion coefficient in z direction, d_{eh} is the deformation potential, $n(0, t)$ is the carrier concentration and $\Delta T(0, t)$ is the temperature change. The analytical calculation shows that the region near surface ($z > 0$) always has time independent strain due to thermal lattice expansion having a microsecond long time relaxation. While the second part of strain is an acoustic wave that propagates away from the free surface with the speed of longitudinal sound v_{ac} [14]. The stress confinement in the absorption depth determines the value of PA magnitude. The condition $\alpha v_{ac}\tau_L < 1$ means that full laser energy is deposited into the PA wave for duration τ_L by the absorption α before it propagates acoustically [15]. If $\alpha v_{ac}\tau_L < 1$, the strong absorption condition is reached and the absorption depth becomes smaller than the area element which can propagate acoustically. The theoretical consideration shows that the PAS magnitude then starts to decrease inversely with α for this case [10].

In usual detection schemes, a piezoelectric transducer is placed on the sample back side to detect the time-dependent strain of acoustic wave [12]. In our experiment, we used the Schlieren approach which as a method was first described for application in liquids and gases [10]. A focused probe CW beam is directed to the lateral side of the semiconductor slab at a certain distance from the excited surface. The knife edge is inserted and cuts off half of the probe beam between two collecting lenses, as shown in Fig. 1(b). This allows detecting a small variation of the refractive index induced by the passage of pressure at a cylindrical acoustic wave [10]

$$n(p,T) = n_0(T) + \left.\frac{\partial n(T)}{\partial p}\right|_{p=0} p, \qquad (2)$$

where n_0 indicates the normal refractive index at temperature T and at zero additional pressure p. For a small temperature rise we may assume the second term on the right-hand side of Eq. (2) being independent of temperature. Furthermore, a small change of the refractive index can be set to be proportional to the pressure

$$n_1(T) = n_1 = \left.\frac{\partial n}{\partial p}\right|_{p=0} p. \qquad (3)$$

The advantage of the Schlieren scheme lies in the possibility of detecting various positions with respect to the excited surface [8, 9]. The theoretical stress profile is shown in Fig. 1(c) and its derivative is given in Fig. 1(d). The value of PAS is represented by relation $A = \Delta I/I_0 \times 100\%$ as indicated. Figure 1(e) presents the experimental time response to laser pulse for the opposite direction of the inserted knife in $TlGaSe_2$. The symmetry of signals indicates the symmetry of compression/expansion paths at unbound surface [14, 16].

4. Results

Figure 2 shows the experimentally obtained PAS with a knife inserted from the side of excited surface in GaAs and $TlGaSe_2$. The similar measurement condition was achieved by maintaining light photon energy slightly above the band gap of each semiconductor, i.e. the energy 1.514 eV that exceeds the direct band gap in the GaAs by 85 meV [16], and 2.296 eV that exceeds the band gap in $TlGaSe_2$ by 151 meV. Both PAS traces contain the first peak (1st) due to generated PA wave travelling from the excited surface to the z position of the probe beam. The 2nd signal is recorded on the wave returning trip after reflection from the back surface. The 3rd signal is from the wave moving in the forward direction after reflection from the front surface, and the 4th one is from the wave moving in the back direction after reflection from the back surface again. Up to hundred echoes can be measured in such a way (not shown). Note that PAS shape distortion as a result of acoustic energy dissipation occurs in 2D-$TlGaSe_2$ slabs only after about 10–20 round trips [8, 13]. This indicates optical qualities of surfaces comparable

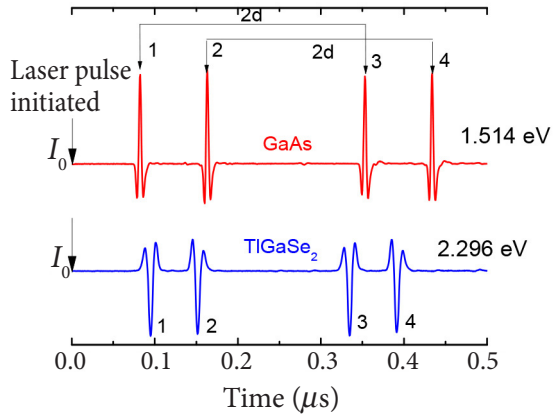

Fig. 2. Comparison of PAS in GaAs and $TlGaSe_2$ obtained for the excitation normal to the (100) surface at 295 K with laser excitation by photons with energy above the band gap and fluence F = 2 mJ/cm^2. Probe is performed by 1540 μm wavelength light. Coloured online.

to a mirror like surface of the GaAs slab. From the time interval between signal peaks 1–3 and 2–4 (Fig. 2) the wave velocity is determined as given in Table 1. The values in the range 300–77 K for $TlGaSe_2$ well correspond to the literature results [8]. The acoustic velocity abruptly jumps due to sequential phase transitions to the low-temperature ferroelectric phase in the 120–106 K range [8]. As shown in Table 1, determined v_{ac} (100) in GaAs also well agrees with literature data. Such agreement adds considerable support for the validity of the Schlieren detection technique.

In the next two figures we depict PAS traces in a wide spectral range and laser pulse fluence F at temperature 295 and 77 K. We should note that in $TlGaS_2$ a very low carrier diffusion exists across the layers [4]. Thus, the excitation volume in the thermoelastic and deformation mechanism is expected to be the same, while in the GaAs excited carriers are free to diffuse into the sample depth. Then the phenomenon of energy conversion to PAS in this case is quite complicated.

Figure 3(a) shows three measurements of PAS in $TlGaSe_2$ at F = 6.3 mJ/cm^2 after excitation with photon energies above the indirect band gap equal to 2.04 eV and two ones with energy below it. The signals after excitation above the band gap remain symmetrical, no shape distortions are observed up to 35 mJ/cm^2 fluence. This can be qualitatively explained that no nonlinear effects associated with optical generation and carrier recombination were detected. In Fig. 3(b) we demonstrate the agreement of PAS (in magnitude A) in comparison with the optical absorption coefficient detected from spectroscopic measurements. The PAS correctly presents the absorption edge up to value $\alpha = 7 \cdot 10^3$ cm^{-1} where the stress confinement condition approaches a limit, i.e. $\alpha v_{ac} \tau_L = 1$. Also, the PAS starts to decrease at higher energies as ~$1/\alpha$. The PAS nearly linearly increases with fluence in all measured spectral ranges. A few of such dependences are shown at 77 K. Due to

Table 1. Parameters of GaAs and $TlGaSe_2$ extracted from the photo-acoustic response. Data with asterisks (*) (red online) obtained in the current work.

Parameter	GaAs		$TlGaSe_2$	
	295 K	77 K	295 K	77 K
Longitudinal sound velocity v_{ac} (cm/s) along axis (100)	$4.719 \cdot 10^5$ 17] $4.770 \cdot 10^5$ (*)	$4.766 \cdot 10^5$ [17] $4.81 \cdot 10^5$ (*)	$2.6 \cdot 10^5$ [8] $2.53 \cdot 10^5$ (*)	$2.66 \cdot 10^5$ [8] $2.55 \cdot 10^5$ (*)
Thermal expansion coefficient β (1/K) along axis (100)	$5.73 \cdot 10^{-6}$ [17]	~$1 \cdot 10^{-6}$ [17]	$1 \cdot 10^{-6}$ [20]	$3 \cdot 10^{-6}$ [20]
Heat capacity C_p (J/g·K)	0.3 [17]	0.15 [17]	0.665 [23]	0.52 [23]
Gruneisen parameter, G	0.425 [17]	0.2 [17]	0.1 [8]	–
Refractive indexes	n = 3.36 [21] at 0.7 eV	–	N_0 = 2.51[20] at 0.8 eV	–
Change of refractive index with hydrostatic pressure $(1/n)\cdot(dn/dp)$ (1/GPa)	$-4.5 \cdot 10^{-3}$ [21] at 0.7 eV	–	$\geq 1.27 \cdot 10^{-2}$ (*) at 0.8 eV	–

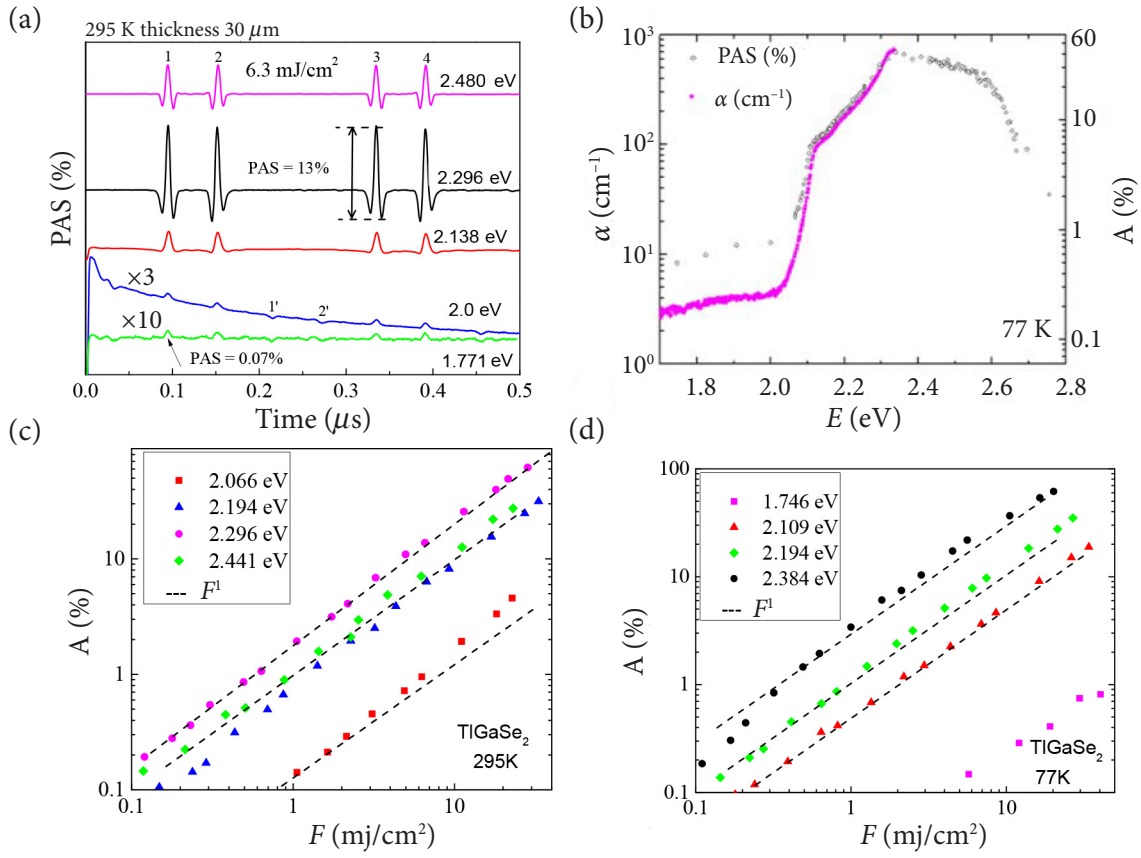

Fig. 3. PAS in $TlGaSe_2$. (a) The traces of PAS after laser pulses with different photon energy at fluence F = 6.3 mJ/cm^2 and T = 295 K. Pay attention to the appearance of new signals (labelled as 1′ and 2′) after excitation with photon energy 2.0 and 1.771 eV, below the band gap. The explanation is given in the text. (b) The spectral response of PAS (in magnitude A) in comparison with the absorption spectrum at 77 K. The fluence dependences of PAS at 295 K (c) and 77 K (d) fitted by linear relation F^1 as indicated by the dashed line. Coloured online.

a low absorption value this range is relatively wide. A very high magnitude of 70% was reached with no sign of PAS saturation. However, it must be noted that after excitation by photons with energy below the band gap (E < 2.04 eV at 77 K) we still observe the PAS of sufficient strength (Fig. 3(b)). Moreover, in this range new signals occur as labelled 1′ and 2′ in Fig. 3(a) after excitation at 2.0 and 1.771 eV. Existence of these signals is not explicable on the basis of the usual generation mechanism. Discussion of the possible cause of this phenomenon will be provided in Section 6.

The PAS obtained in GaAs are presented in Fig. 4. The PAS in magnitude A increases with exciting energy at 295 K in accordance with the steep rise of the absorption coefficient; data of α presented in Fig. 4(a) are taken from [17]. The PAS reaches its maximum at exciting energy wherein $\alpha = 1.5 \times 10^3$ cm^{-3} and the confinement condition exceed the unity. For large energies above 1.425 eV the absorption depth becomes smaller than the area element which can propagate acoustically, therefore acoustic pressure starts to decrease following dependence ~$1/\alpha$ [10]. Previously, the PA pressure measurements in GaAs were performed after the similar nanosecond laser duration with a piezoelectric transducer attached to the back of the sample and were reported by Song et al. [12]. Song's results check well with our PAS measurement in the energy range 1.4–1.75 eV as shown in Fig. 4(b). Such a good coincidence indicates that both techniques produce identical results. The maximum PA pressure of 0.8 mbar occurs at 1.425 eV, where the limiting condition $\alpha v_{ac} \tau_L = 1$ is fulfilled. Figure 4(c) presents the PAS measured in GaAs slab over a wide range of fluence at 295 K. The linear dependence

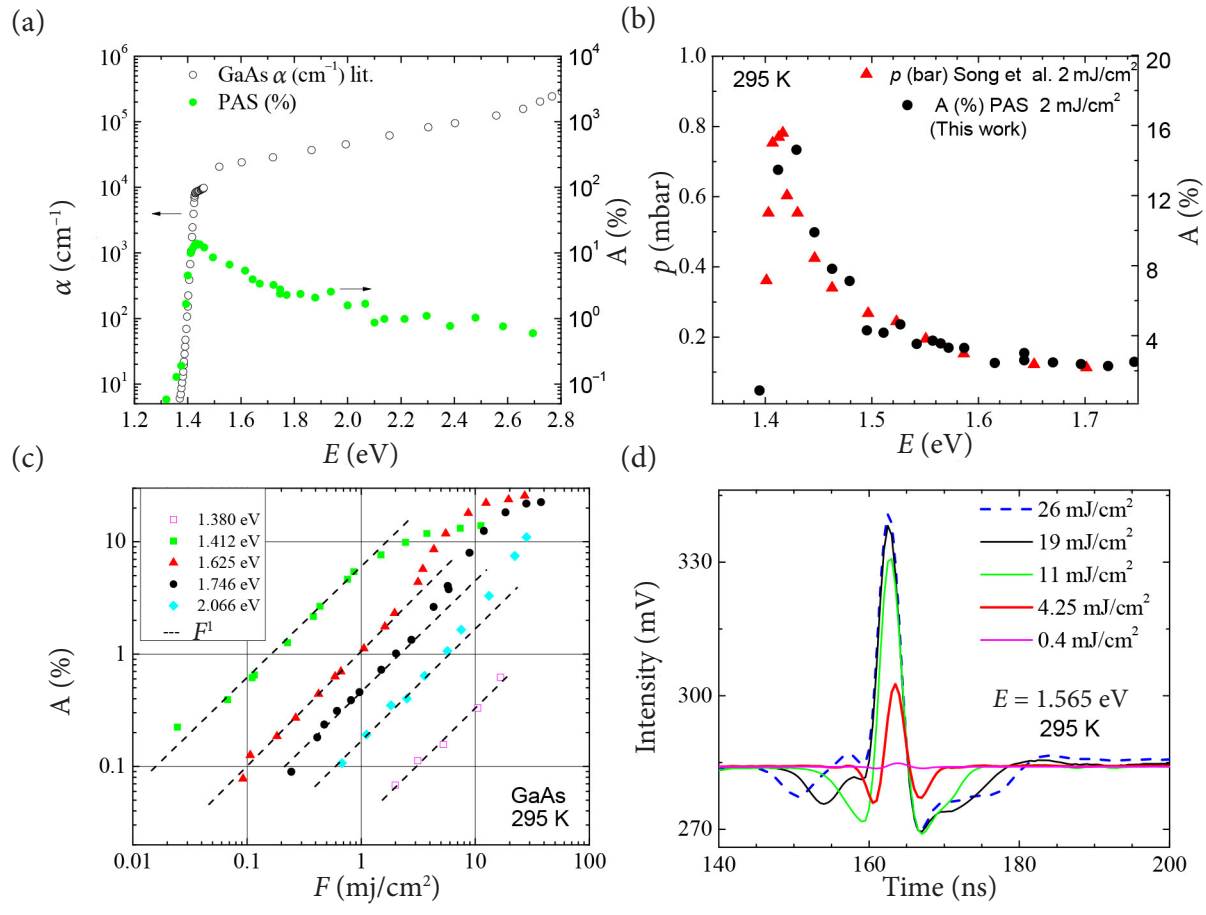

Fig. 4. PAS in GaAs. (a) Comparison of the PAS magnitude and absorption coefficient [17] spectral dependences at 295 K. The stress confinement reaches unity at absorption $\alpha = 1.5 \cdot 10^3$ cm^{-1}. (b) Comparison of the PAS and the acoustic pressure from Song et al. article [12]. (c) The fluence dependences of PAS after excitation with different energy photons. The dashed line indicates linear growth. The superliner growth above the dashed line is due to the TPA process. PAS saturation observed is caused by the band gap filling. (d) PAS temporal profiles at 1.565 eV excitation with increasing fluence and change of their shape due to occurrence of nonlinearities. Coloured online.

clearly prevails as indicated by dashed lines ~F^1. However, the sublinear PAS rise above the dashed line is evident at larger fluence in the energy range 1.625–2.066 eV. Such super-linearity can be attributed to filling of a higher L valley of the conduction band by two-photon absorption (TPA). Moreover, with the following increase of fluence, PAS start to saturate at A = 10–20%. The fluence threshold in saturation shifts down as excitation energy approaches the direct band gap. This effect is well documented for GaAs when the generation level exceeds the e–h density of 10^{18} cm^{-3}. It happens due to the electron state filling by direct band gap transitions, the so-called Burstein–Moss effect. At 77 K we have obtained the measured PAS saturation to its value of A = 1–2% (not shown). The lower value at 77 K can be explained by strong carrier diffusion from the excitation volume, based on a high carrier mobility, which in pure GaAs is $\mu_e > 10^5$ cm^2/Vs and $\mu_h = 10^4$ cm^2/Vs [17]. As a consequence, the induced absorption bleaching occurs with a small energy transfer to the acoustic wave.

All the nonlinear effects in GaAs are manifested by temporal distortion of the PA wave after excitation by 1.565 eV photons at T = 295 K, as illustrated in Fig. 4(d) with growing fluence. In this way, wings in the PAS shape indicate a different spread of PA pressure on variable depths, determined by competitive nonlinear processes. The complicated phenomena are in agreement with state-of-the-art PA measurements in GaAs where it can be resolved using shorter laser pulses in femtosecond-to-picosecond ranges [11].

5. Photo-darkening in $TlGaSe_2$

In Fig. 5 we present the results obtained in $TlGaSe_2$ after CW beam focusing on the (100) surface. Up to 25 samples of different growth were tested, and the darkening phenomenon was observed in all of them after 633, 671 and 861 nm wavelength irradiation. The used longer wavelengths (1540,

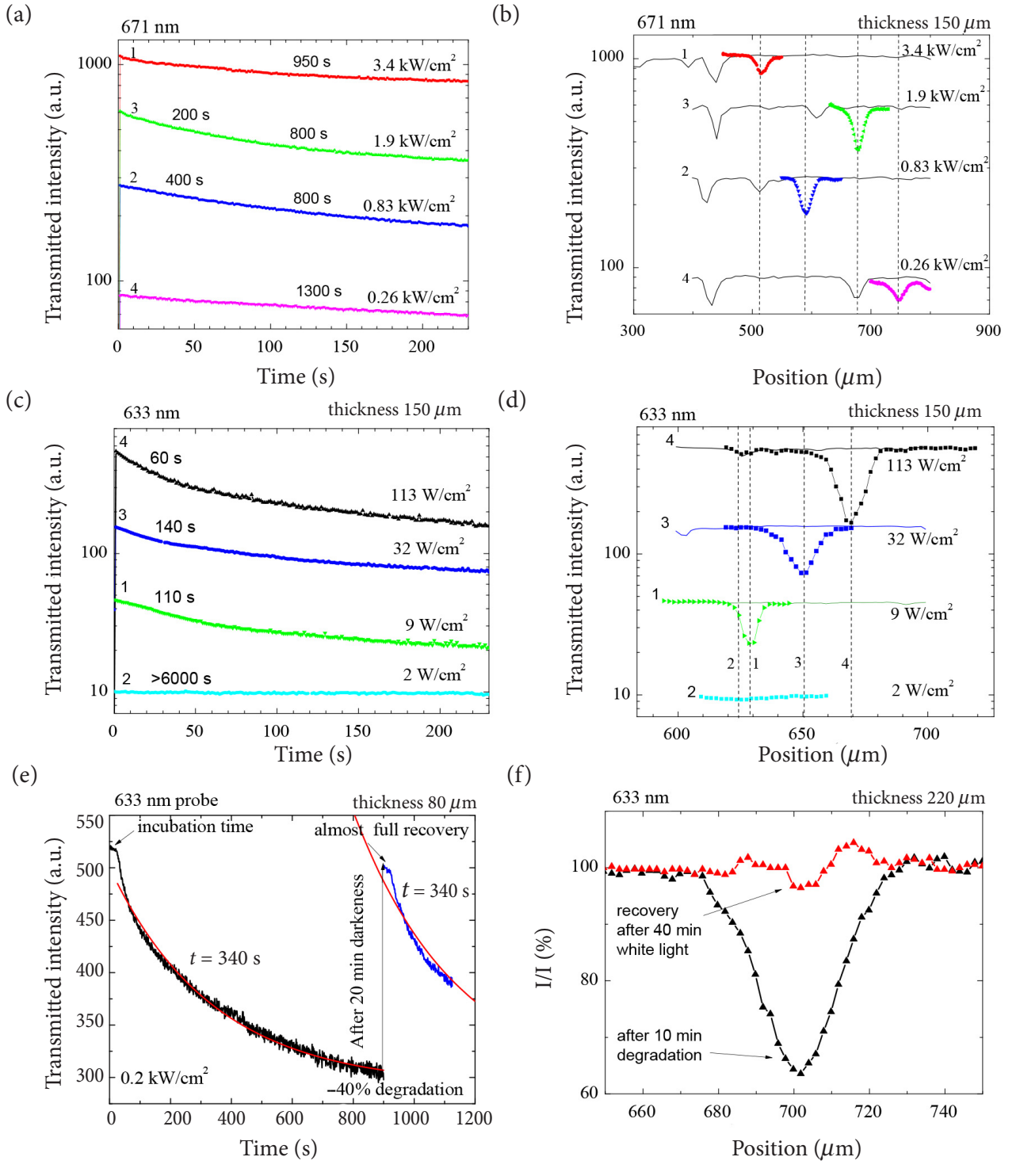

Fig. 5. Photo-darkening kinetics in the $TlGaSe_2$ platelets at 671 and 633 nm wavelength at 295 K. Left-hand panels show the kinetics with the indicated speed of degradation time. Right-hand panels show the transmitted intensity profiles measured immediately after darkening (a solid line with points) and after recovery ((b, d) thin lines, (f) upper line with light triangles). Coloured online.

1300, 980 nm) did not show such phenomenon. A few responses after 633 and 671 nm irradiation with different power density obtained on the fresh area of the sample are shown in Fig. 5(a, c). As indicated, the time of degradation reduces with increasing the power density and, in the extreme, it can reach a second. In some cases, after a low/moderate power the photo-darkening process does not start immediately but after a certain incubation period, typically within 1–10 s (Fig. 5(e)). For a low power, the optical darkening recovery after keeping the sample during minutes in the darkness was detected (Fig. 5(e, f)). This phenomenon was observed on about 80% of the investigated cases. However, the recovery time depends on the darkening level produced, and the duration period and a number of irradiation cycles. The darkening of a similar strength was also observed at 77 K.

We tested the darkening process by additional illumination of a strong white light from a 200 W lamp (spectrum including above the band gap wavelength) which increases the background excitation of the sample. The lamp light was focused to ~2 mm diameter spot and directed either to the front surface at a slight angle or perpendicularly to the lateral surface of the sample. In these cases, sample degradation became longer but the effect was not strong. The recovery process was also enhanced by incandescence white light (not shown).

General features of the darkening process can be summarized as follows. The recovery process of darkening is obvious after irradiation with a low power. After higher one the darkening recovers only partly. The darkened spot can be defined by another scan, as illustrated in Fig. 5(b, d, f). Furthermore, such spot can be detected using the light with IR wavelength which itself does not produce changes. After the high power (671 nm, range 5–50 kW/cm^2) permanent photo-darkening was detected. It seems that the power threshold depends basically on the position on the $TlGaSe_2$ platelet rather than on different samples and their thicknesses. We have found that irradiation during 60 s with comparable power density ~0.2 kW/cm^2 produced degradation of intensity 90% at 633 nm (1.96 eV) while only ~10% at 671 nm (1.83 eV) and about ~5% at 861 nm (1.44 eV). Thus, the degradation process is particularly strong if the illumination energy approaches the band gap.

In Fig. 6 we present the pictures of damaged places obtained by irradiation of extreme CW powers. The samples were scanned using motion of the cryostat. The scanning was produced in the measurement mode, i.e. a fast sub-second move a distance from one step position into the next one (determined by computer) and ~3 s holding time in each step position. Figure 6(a) shows the extreme case (A) where local explosion is produced on the scanning line while the sample has been residing in vacuum. As seen, the hollow line is drilled. When the excitation is produced in air, the explosion produces evaporated material remnants spread around in the sample, such as spot B in Fig. 6(a). In Fig. 6(b) we present the case of irradiations by less power in air. A few lines perpendicular/parallel to each other were produced. The zoomed view

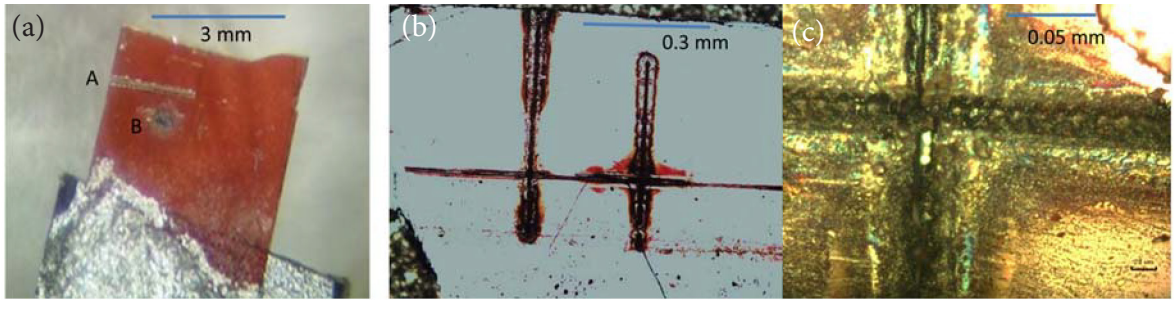

Fig. 6. $TlGaSe_2$ degradation at high power density of CW light by illumination of the moving sample (see explanation in the text). (a) At 633 nm (1.96 eV) irradiation: (A) in vacuum the material is completely evaporated and only empty line is left; (B) in air the crater is formed with surroundings of remnants spread around. (b) Several lines produced by 671 nm (1.85 eV) irradiation in air; scans in the perpendicular/parallel direction to each other. (c) A zoomed view of the two-line crossing from the (b) panel on an enlarged scale. Note that pits represent craters at the position of sample stop within 3 s before faster movement to the next stop position. Coloured online.

of them in Fig. 6(c) indicates that crater spots were created where the movement of the sample was stopped for 3 s between steps. It must be noted that at power densities below the band gap there was not any photo-darkening in GaAs while the absorption coefficient in GaAs is by factor 5 stronger than that in $TlGaSe_2$. We observed no photo-darkening in isotropic semiconductors: Si, GaP and CdS. Thus, we conclude that the phenomenon in the $TlGaSe_2$ sample is closely related to the two-dimensional structure of this material.

6. Discussion

It should be emphasized that the parameters which determine the amplitude and polarity of PAS wave are the deformation potential d_{DP} and the refraction coefficient dependence on pressure dn/dp, both acting as a transfer function in the energy conversion. The laser energy as deposited to the sample lattice is determined by heat capacity C_p (J/g·K) and averaged Gruneisen parameter $G = \beta(v_{ac})^2/C_p$ which represents a measure of heat to acoustic energy conversion (see Table 1). However, in $TlGaSe_2$ parameter dn/dp is not determined by independent experiment. From the PAS measurements presented in Fig. 2 we find that the A polarity in $TlGaSe_2$ and GaAs obtained within the same experimental conditions is certainly the reverse of each other.

Thus, we assume that the sign of dn/dp in $TlGaSe_2$ is positive as is customarily observed in amorphous and 2D semiconductors [18]. And conversely, the negative signs of this parameter are observed in most isotropic crystalline semiconductors, including GaAs for dn/dp = $+4.5 \cdot 10^{-3}$ [21]. Assuming the positive sign for $TlGaSe_2$ and assigning the experimental values of dn/dp as in van der Waals 2D semiconductors, like InSe and GaSe (dn/dp = $-4.5 \cdot 10^{-2}$ [19]), we estimate the deformation potential of $TlGaSe_2$ as d_{eh} = 3 eV in agreement with the value derived by Allakhverdiev et al. [20]. This value is three times smaller than the known deformation potential of GaAs d_{eh} = 10 eV [17]. Hence, a high PAS in $TlGaSe_2$ is caused primarily by a large dn/dp value (Table 1). It is known that the refraction index below the band gap is controlled by interlayer spacing where interlayer Tl 6p and Se 4p electronic orbitals determine the bound states at the edges of conduction and valence band [2, 5, 6]. We also obtained the large PAS in $TlInS_2$ with the same polarity as in $TlGaSe_2$ (not shown). Hence it follows that the presented dn/dp value and its sign in $TlGaSe_2$ are inherent to dichalcogenides 2D structure which possesses interlayer flexibility. On the other hand, the low absorption coefficient above the band gap and the absence in band gap filling exhibit the corresponding linearity of PAS with fluence. Such property can be exploited for optical signal conversion or switching. For example, when a CW laser beam travels through a crystal in controlling optical circuit, a perpendicular laser induces the deflection pulse of CW beam for automatic recording of the on/off state in an optical line.

Another peculiarity obtained in $TlGaSe_2$ is occurrence of signals 1′, 2′… after excitation with energy below the band gap (Fig. 3(a)). Such behaviour was investigated explicitly using the two-laser pulse excitation from the opposite surfaces simultaneously [8]. These measurements allow one to draw a conclusion that 1′ signal is generated near the back surface (contrary to signal 1 generated near the front one). Its polarity is determined by PAS from the back to the front surface. Then signal 2′ after PAS reflection is generated from the front surface on a way back when crossing the probe beam position. Both signals can interfere at a certain probing depth (note that signal 2 is generated on a way towards the front surface). Both shapes of waveforms are narrow (about 10 ns) and are caused by a probe beam diameter and 2 ns duration of the laser pulse. This does not allow one to resolve the actual generation depth. However, they are sufficiently narrower than the inverse absorption coefficient $1/\alpha > 0.5$ mm. In other words, acoustic energy could not generate such narrow PAS wave by uniform thermoelastic-deformation conversion. Moreover, the PAS in $TlGaSe_2$ at low pump energy is factor 3 stronger than the corresponding absorption (see Fig. 3(b)). No sub-band-gap PAS were registered in the GaAs. All these features indicate that the mechanism of PAS generation in $TlGaSe_2$ differs from the ordinary thermoelastic-deformation conversion. We suggest that the planar stacking faults are responsible for the occurrence of these PAS.

It is known that PSFs are quite common defects in Tl dichalcogenides due to gliding of one structural layer by 1/2 lattice unit in reference to

the neighbouring layer and keeping the same unit cell. The PSFs were identified by X-ray scattering in the $TlGaSe_2$ compound, and it was concluded that a shift occurs in this crystal every four layers on the average [22]. It is known that PSFs also participate in the sub-band-gap absorption spectrum. The reported lattice expansion in $TlGaSe_2$ shows a strong anisotropy which is increasing at the phase transition range 100–120 K [20], and also can be resulting from PDFs. Such knowledge allows one to suggest that PDFs located near the surface react to the deformation energy stronger than those inside the crystal. The presence of surface produces a sufficiently high interlayer flexibility. We speculate that such PSF transformation in the near surface region provides the specific PAS generation. However, the energy of the acoustic wave is negligible compared with the internal crystal energy.

According to the microscopic model presented in Ref. [6] the excitation can produce optical filling of deep different defect states which are situated on PSF edges as defect lines. Presence of such defects (dangling bonds, inclusions, clusters) is important since they stabilize the formation of the total PSF structure in 2D [6]. Thus, we assume that the absorption process below the gap is responsible for filling PSF edge defects. If defect filling is completed by a sufficiently strong CW irradiation, the flexibility in PSF movement increases. Such movement generates the Stark field in nearby layers near the surface. If the Stark field is not strong, it can be reduced by accumulating free charges from the bulk or from the surface (either in darkness or by addition of white light). However, if the Stark field is strong enough, it can produce progressive multiplication into next layers by spontaneous polarization of the whole sample. We note that the Stark field, which was generated in the $TlInS_2$ sample before [6], was produced by strong above-band-gap laser pulse excitation with e–h excess pairs in $>10^{18}$ cm^{-3} density. The estimate in Stark fields needed to produce explosion in $TlGaSe_2$ should be in a range of MV/cm^2. Under typical ablation processes the lattice thermal heating is typically reached during the laser pulse at melting temperature. This is not a present case where thermal heating is expected to be moderate by the below-band-gap excitation. According to our knowledge, no observation of the darkening process has been published before in the dichalcogenides for the sub-gap excitation spectral range. Another kind of photo-darkening processes are those mentioned in literature in the semiconductor-doped glasses [24] or in the semiconductor-doped dielectrics [25]. These processes are produced by laser pulses at low absorptive media, however they also require an intense pulse excitation. The processes are ruled typically by carrier escape from a semiconductor nanoparticle into a surrounding medium by obtaining the energy from the local Auger recombination event [26].

7. Conclusions

We have shown that the Schlieren technique revealed the PAS amplitude in 2D-$TlGaSe_2$ which is enhanced by a high dn/dp value and negative sign in the (100) direction. The PAS signals for the above-band-gap excitation are symmetrical and undistorted, they occur in a wide spectral range with magnitude linearly increasing up to 70%. This is in contrast to the GaAs where PAS obey nonlinear optical phenomena and PAS profile distortion by nonlinear optical processes.

For the below-band-gap excitation in $TlGaSe_2$ we observe the PAS signals generated on front and back surfaces that can be explained by the flexibility of PSF presence in the 2D structure. In the spectral range below the band gap (1.4–2.0 eV) we demonstrate the generation of giant Stark effect. At moderate powers, the photo-darkening effect occurs with increasing light density and with reducing degradation time from hundreds to few seconds. Recovery effects of darkening are also detected. The highest darkening effect observed is just in the spectrum range below the band gap. At higher CW excitation, the Stark effect occurs in seconds and produces local material explosion or damage. More experiments are needed to use such process in layered Tl-chalcogenide semiconductors and to obtain practical application for this behaviour.

Acknowledgements

We would like to thank the Swedish Institute for financial supports during the previous decade and prof. Jan Linnros for help and discussions at the Royal Institute of Technology of Stockholm.

References

[1] A.M. Panich, Electronic properties and phase transitions in low-dimensional semiconductors, J. Phys. Condens. Matter **20**, 293202 (2008).

[2] S. Johnsen, Z. Liu, J.A. Peters, J.-H. Song, S.C. Peter, C.D. Malliakas, N.K. Cho, H. Jin, A.J. Freeman, B.W. Wessels, and M.G. Kanatzidis, Thallium chalcogenide-based wide-band-gap semiconductors: $TlGaSe_2$ for radiation detectors, Chem. Mater. **23**, 3120 (2011).

[3] K.A. Yee and Th.A. Albright, Bonding and structure of $TIGaSe_2$, J. Amer. Chem. Soc. **113**, 6474 (1991).

[4] K. Gulbinas, V. Grivickas, and V. Gavryushin, Anisotropy of band gap absorption in $TlGaSe_2$ semiconductor by ferroelectric phase transformation, Appl. Phys. Lett. **10**, 5242107 (2014).

[5] M.-H.Yu. Seyidov, R.A. Suleymanov, F. Sale, and E. Balaban, Enhanced exciton photoconductivity due to build-in electric field in $TlGaSe_2$ layered semiconductor, J. Appl. Phys. **116**, 213702 (2014).

[6] V. Grivickas, P. Ščajev, V. Bikbajevas, O.V. Korolik, and A.V. Mazanik, Carrier dynamics in highly excited $TlInS_2$: evidence of 2D electron–hole charge separation at parallel layers, Phys. Chem. Chem. Phys. **21**, 2102 (2019).

[7] V. Grivickas, K. Gulbinas, V. Gavryushin, V. Bikbajevas, O.V. Korolik, A.V. Mazanik, and A.K. Fedotov, Room-temperature photoluminescence in quasi-2D $TlGaSe_2$ and $TlInS_2$ semiconductors, Phys. Status Solidi RRL **8**, 639 (2014).

[8] V. Grivickas, V. Bikbajevas, K. Gulbinas, V. Gavryushin, and J. Linnros, Strong photoacoustic oscillations in layered $TlGaSe_2$ semiconductor, Phys. Status Solidi B **244**, 4624 (2007).

[9] V. Grivickas, V. Bikbajevas, K. Allakhverdiev, and J. Linnros, Two-photon absorption in GaSe, J. Phys. Conf. Ser. **100**, 042008 (2008).

[10] M.W. Sigrist, Laser generation of acoustic wave in liquids and gases, J. Appl. Phys. **60**, R83 (1986).

[11] E.S.K. Young, A.V. Akimov, R.P. Campion, A.J. Kent, and V. Gusev, Picosecond strain pulses generated by a supersonically expanding electron-hole plasma in GaAs, Phys. Rev. B **86**, 155207 (2012).

[12] K. Song, H. Cha, J. Lee, and I.A. Veselovskii, Application of optical parametric oscillators to photoacoustic studies in semiconductors, Appl. Phys. B **61**, 547 (1995).

[13] K. Gulbinas, *Photoelectrical and Optical Properties of Indirect Bandgap Semiconductors*, PhD Thesis (Vilnius University, 2015).

[14] C. Thomsen, H.T. Grahn, H.J. Maris, and J. Tauc, Surface generation and detection of phonons by picosecond light pulses, Phys. Rev. B **34**, 4129 (1986).

[15] J. Zelewski and R. Kudrawiec, Photoacoustic and modulated reflectance studies of indirect and direct band gap in van der Waals crystals, Sci. Rep. **7**, 15365 (2021).

[16] B. Sullivan and A.C. Tam, Profile of laser-produced acoustic pulse in a liquid, J. Acoust. Soc. Am. **75**, 437 (1984).

[17] A. Dargys and J. Kundrotas, *Handbook on Physical Properties of Ge, Si, GaAs and InP* (Science and Encyclopedia Publishers, Vilnius, Lithuania, 1994).

[18] B. Weinstein, R. Zallen, M. Slade, and A. deLozanne, Photoelastic trends for amorphous and crystalline solids of differing network dimensionality, Phys. Rev. B **24**, 4652 (1981).

[19] F.J. Manjon, Y. van der Vijver, A. Segura, and V. Muñoz, Pressure dependence of the refractive index in InSe, Semicond. Sci. Tech. **15**, 806 (2000).

[20] K.R. Allakhverdiev, T.G. Mammadov, R.A. Suleymanov, and N.Z. Gasanov, Deformation effects in electronic spectra of the layered semiconductors $TlGaS_2$, $TlGaSe_2$ and $TlInS_2$, J. Phys. Condens. Matter **15**, 1291 (2003).

[21] S. Adachi, *GaAs and Related Materials, Bulk Semiconductors and Superlattice Properties* (World Scientific, Singapore, 1994).

[22] D.F. McMorrow, R.A. Cowley, P.D. Hatton, and J. Banys, The structure of the paraelectric and incommensurate phases of $TlGaSe_2$, J. Phys. Condens. Matter **2**, 3699 (1990).

[23] K.R. Allakhverdiev, M.A. Aldzanov, T.G. Mamedov, and E.Yu. Salaev, Anomalous behaviour of the Urbach edge and phase transitions in $TlGaSe_2$, Sol. St. Commun. **58**, 295 (1986).

[24] M. Kull, J.L. Coutaz, G. Manneberg, and V. Grivickas, Absorption saturation and photodarkening in semiconductor-doped glasses, Appl. Phys. Lett. **54**, 1830 (1989).

[25] J. Linnros, N. Lalic, A. Galeckas, and V. Grivickas, Analysis of the stretched exponential photoluminescence decay from nanometer-sized silicon crystals in SiO_2, J. Appl. Phys. **86**, 6128 (1999).

[26] P. Roussignol, M. Kull, D. Ricard, F. de Rougemont, R. Frey, and C. Flytzanis, Time-resolved direct observation of Auger recombination in semiconductor-doped glasses, Appl. Phys. Lett. **51**, 1882 (1987).

AKUSTINIS 2D-$TlGaSe_2$ IR GaAs PUSLAIDININKIŲ FOTOATSAKAS BEI OPTINĖS YPATYBĖS

V. Grivickas [a], K. Gulbinas [a], V. Bikbajevas [a], P. Grivickas [b]

[a] *Vilniaus universiteto Fotonikos ir nanotechnologijų institutas, Vilnius, Lietuva*

[b] *Lawrence'o Livermoro nacionalinė laboratorija, Livermoras, Kalifornija, JAV*

Santrauka

Naudodami lazerio impulsus tyrėme fotoakustines 2D-$TlGaSe_2$ ir GaAs puslaidininkių savybes. Taip pat atlikome fotopatamsėjimo eksperimentus, naudodami pastovaus veikimo fokusuotą apšvitinimą su mažesne nei $TlGaSe_2$ sugerties kraštas kvanto energija. Parodyta, kad fotoakustiniai signalai, generuojami lazerio kvanto energija, virš $TlGaSe_2$ sugerties krašto yra daug stipresni, o nuo sužadinimo lygio – tiesiški, GaAs yra iškraipomi kelių netiesinių optinių procesų. Atlikti palyginimai atskleidė būdingus $TlGaSe_2$ parametrus, atsakingus už šį reiškinį. Tai didelis lūžio rodiklio pokytis tarpsluoksnio slėgio (100) kryptimi ir neigiamas pakitimo ženklas, taip pat esant nedideliam sugerties koeficientui ir nestebint energetinių būsenų užpildymo. Šios savybės garantuoja stabilų lazerio energijos konversijos lygį į akustinius signalus per termoelastinį–deformacinį fotoatsaką. Žemiau energijos krašto aptikome naujus akustinius signalus $TlGaSe_2$ bandiniuose. Matavimai fokusuotos nuolatinės veikos spinduliais šioje kvantų srityje parodė atsirandantį didelį Štarko efektą, kuris indukuoja $TlGaSe_2$ bandinių tamsėjimą ir esant dideliam energijos tankiui sukelia lokalinę medžiagos degradaciją arba sprogimą apšvitintose srityse. Darbo rezultatai leidžia manyti, kad planariniai sanglaudos defektai, būdingi $TlGaSe_2$ sluoksnių struktūroms, yra atsakingi už pasirodžiusią sluoksnių poliarizaciją ir šių savaiminių reiškinių atsiradimą.